We are IntechOpen, the world's leading publisher of Open Access books Built by scientists, for scientists

6,900
Open access books available

186,000
International authors and editors

200M
Downloads

Our authors are among the

154
Countries delivered to

TOP 1%
most cited scientists

12.2%
Contributors from top 500 universities

CLARIVATE ANALYTICS
BOOK CITATION INDEX
INDEXED

WEB OF SCIENCE™

Selection of our books indexed in the Book Citation Index
in Web of Science™ Core Collection (BKCI)

Interested in publishing with us?
Contact book.department@intechopen.com

Numbers displayed above are based on latest data collected.
For more information visit www.intechopen.com

Dynamic Responses and Active Vibration Control of Beam Structures Under a Travelling Mass

Bong-Jo Ryu and Yong-Sik Kong

Additional information is available at the end of the chapter

1. Introduction

The dynamic deflection and vibration control of an elastic beam structure carrying moving masses or loads have long been an interesting subject to many researchers. This is one of the most important subjects in the areas of structural dynamics and vibration control. Bridges, railway bridges, cranes, cable ways, tunnels, and pipes are the typical structural examples of the structure to be designed to support moving masses and loads.

While the analytical studies on the dynamic behavior of a structure under moving masses and loads have been actively performed, a small number of experimental studies, especially for the vibration control of the beam structures carrying moving masses and loads, have been conducted. It is, therefore, strongly desired to conduct both analytical and experimental studies in parallel to develop the algorithm that controls effectively the vibration and the dynamic response of structures under moving masses and loads.

The dynamic responses and vibrations of structures under moving masses and loads were initially studied by (Stokes, 1849; Ayre et al., 1950) who tried to solve the problem of railway bridges. This type of study has been actively performed by employing the finite element method (Yoshida & Weaver, 1971). (Ryu, 1983) used the finite difference method to study the dynamic response of both the simply supported beam and the continuous beam model carrying a moving mass with constant velocity and acceleration. (Sadiku & Leipholz, 1987) utilized the Green's function to present the difference of the solutions for the moving mass problem without and with including the inertia effect of a mass. (Olsson, 1991) studied the dynamic response of a simply supported beam traversed by a moving object of the constant velocity without considering the inertia effect of moving mass. (Esmailzadeh & Ghorash, 1992) expanded Olsson's study by including the inertia effect of the moving mass. (Lin, 1997) suggested the effects of both centrifugal and Coliolis forces should be taken into account to obtain the dynamic deflection. (Wang & Chou, 1998) conducted nonlinear

vibration of Timoshenko beam due to a moving force and the weight of beam. Recently, (Wu, 2005) studied dynamic analysis of an inclined beam due to moving loads.

Most studies on the dynamic response of a beam carrying moving mass or loads are analytical, but a small number of experimental investigations are recently conducted in parallel. The studies on the dynamic response of a beam caused by moving masses or loads have been also conducted domestically. For the studies on the vibration control of moving masses or loads, (Abdel-Rohman & Leipholz, 1980) applied the active vibration control method to control the beam vibration caused by moving masses. They applied the bending moment produced by tension and compression of an actuator to the beam when the vibration of a simply supported beam carrying a moving mass occurs. With the active control, the passive control approaches have been proposed in many engineering fields. (Kwon et al., 1998) presented an approach to reduce the deflection of a beam under a moving load by means of adjusting the parameters of a conceptually second order damped model attached to a flexible structures.

Recently, the piezoelectric material has been used for the active vibration control. (Ryou et al., 1997) studied the vibration control of a beam by employing the distributed piezoelectric film sensor and the piezoelectric ceramic actuator. They verified their sensor and actuator system by observing the piezoelectric film sensor blocked effectively the signal from the uncontrolled modes.

(Bailey & Hubbard Jr., 1985) conducted the active vibration control on a thin cantilever beam through the distributed piezoelectric-polymer and designed the controller using Lyapunov's second and direct method. (Kwak & Sciulli, 1996) performed experiments on the vibration suppression control of active structures through the positive position feedback(PPF) control using a piezoelectric sensor and a piezoelectric actuator based on the fuzzy logic. (Sung, 2002) presented the modeling and control with piezo-actuators for a simply supported beam under a moving mass. Recently, (Nikkhoo et al., 2007) investigated the efficiency of control algorithm in reducing the dynamic response of beams subjected to a moving mass. After that, (Prabakar et al., 2009) studied optimal semi-active control of the half car vehicle model with magneto-rheological damper. (Pisarski & Bajer, 2010) conducted semi-active control of strings supported by viscous damper under a travelling load.

In this chapter, firstly, dynamic response of a simply supported beam caused by a moving mass is investigated by numerical method and experiments. Secondly, the device of an electromagnetic actuator is designed by using a voice coil motor(VCM) and used for the fuzzy control in order to suppress the vibration of the beam generated by a moving mass. Governing equations for dynamic responses of a beam under a moving mass are derived by Galerkin's mode summation method, and the effect of forces (gravity force, Coliolis force, inertia force caused by the slope of the beam, transverse inertia force of the beam) due to the moving mass on the dynamic response of a beam is discussed. For the active control of dynamic deflection and vibration of a beam under the moving mass, the controller based on fuzzy logic is used and the experiments are conducted by VCM(voice coil motor) actuator to suppress the vibration of a beam.

2. Theoretical analyses

2.1. Governing equations of a simply supported beam traversed by a moving mass

The mathematical model of a beam traversed by a moving mass is shown in Fig. 1, where l is the length of a beam, v is the velocity of a moving mass, t is time, $w(z,t)$ is the transverse displacement, z and y are the axial and the transverse coordinates, respectively.
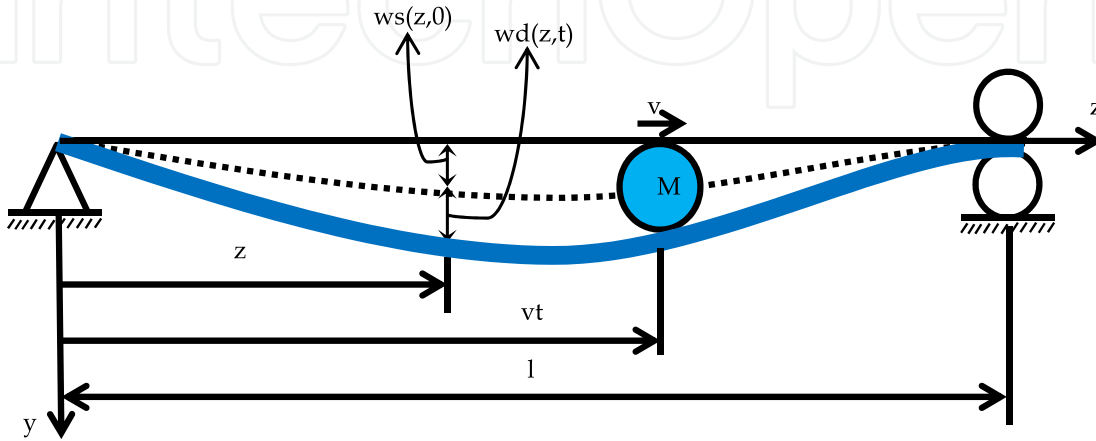
Figure 1. A mathematical model of a simply-supported beam subjected to a moving mass.

The governing equation of the system can be expressed as,

$$EI\frac{\partial^4 w(z,t)}{\partial z^4} + m\frac{\partial^2 w(z,t)}{\partial t^2}$$
$$= mg + Mg\delta(z-vt) - M\left[\frac{\partial^2 w(z,t)}{\partial z^2}v^2 + 2\frac{\partial^2 w(z,t)}{\partial z\partial t}v + \frac{\partial w(z,t)}{\partial z}a + \frac{\partial^2 w(z,t)}{\partial t^2}\right]\delta(z-vt) \tag{1}$$

Where E is Young's modulus of elasticity, I is the cross-sectional area moment of inertia, m is the mass per unit length of a beam, M is the mass of a moving mass, $\delta(z-vt)$ is Dirac delta function, and a is the acceleration of a moving mass. When the mass of a beam is not negligible, the static deflection should be considered. Therefore, the deflection of a beam can be expressed as the sum of the initial static deflection and the dynamic deflection.

$$w(z,t) = w_s(z) + w_d(z,t) \tag{2}$$

Employing Galerkin's mode summation method, the displacement of a beam, $w(\xi,t)$, may be assumed as

$$w_s(\xi) = \sum_{i=1}^{\infty} A_i \phi_i(\xi) \tag{3}$$

$$w_d(\xi,t) = \sum_{i=1}^{\infty} q_i(t) \phi_i(\xi) \tag{4}$$

$$w\left(\xi, t\right) = \sum_{i=1}^{\infty}\left[A_i + q_i(t)\right]\phi_i(\xi) \tag{5}$$

where the dimensionless displacement, $\xi = z / l$. The shape function $\phi_i(\xi)$ is the comparison function and has the general form of

$$\phi_i(\xi)=C_1\sin\beta_i\xi + C_2\cos\beta_i\xi + C_3\sinh\beta_i\xi + C_4\cosh\beta_i\xi \tag{6}$$

For the simply supported beam, the shape function, $\phi_i(\xi)$, may be written as

$$\phi_i(\xi) = \sin i\pi\xi \tag{7}$$

The eigenvalue $\beta_i = i\pi$ and the circular natural frequency w_i have the following relationship

$$w_i^2 = \frac{EI}{m}\left(\frac{\beta_i}{l}\right)^4 \tag{8}$$

From the following equation,

$$\frac{EI}{l^4}\frac{\delta^4 w_s(\xi)}{\delta\xi^4} = mg \tag{9}$$

The static deflection, $w_s(\xi)$, has the following solution form

$$w_s(\xi) = \frac{2mgl^4}{EI\pi^5}\sum_{n=1}^{\infty}\frac{1-(-1)^n}{n^5}\sin n\pi\xi \tag{10}$$

The maximum static deflection δ becomes

$$\delta=w_s\left(\frac{1}{2}\right)=\frac{4}{\pi^5}\frac{mgl^4}{EI}\sum_{n=1}^{\infty}\frac{1}{(2n-1)^5}=\frac{4mgl^4}{EI\pi^5} \tag{11}$$

Substituting the solution of Eq. (5) into Eq. (1) and performing inner product the shape function of $\phi_n(\xi)$ and rearranging provides the equation of motion as

$$\begin{aligned}
\ddot{q}_n(t)+\frac{EI}{m}\left(\frac{n\pi}{l}\right)^4 q_n(t) &= \frac{2gM}{ml}\sin n\pi v^*t - \frac{2M}{ml}\sum_{i=1}^{\infty}\left[\left\{\ddot{q}_i(t)-(i\pi v^*)^2 q_i(t)\right\}\sin i\pi v^*t\right.\\
&\quad+\left\{2i\pi v^*\dot{q}_i(t)+i\pi a^* q_i(t)\right\}\cos i\pi v^*t\right]\sin n\pi v^*t\\
&\quad+\frac{4M}{ml}\frac{mgl^4}{EI\pi^5}\left[(\pi v^*)^2\sum_{i=1}^{\infty}\frac{1-(-1)^i}{i^3}\sin i\pi v^*t\right.\\
&\quad\left.-\pi a^*\sum_{i=1}^{\infty}\frac{1-(-1)^i}{i^4}\cos i\pi v^*t\right]\sin n\pi v^*t
\end{aligned} \tag{12}$$

where, the dimensionless variables and parameter are defined as

$$\gamma = \frac{M}{ml}, \ \delta = \frac{4mgl^4}{EI\pi^5}, \ \tau = \frac{\omega_1}{\pi} t, \ v_0 = \frac{v}{v_{cr}} = \frac{\pi v^*}{\omega_1^2}, \ a_o = \frac{\pi^2 a^*}{\omega_1^2}, \ \varphi_n = \frac{q_n}{\delta}$$ (13)

Eq. (12) can be expressed in matrix form as

$$\left[M(\tau)\right]\left\{\ddot{\varphi}(\tau)\right\} + \left[C(\tau)\right] + \left\{\dot{\varphi}(\tau)\right\} + \left[K(\tau)\right]\left\{\varphi(\tau)\right\} = \left\{f(\tau)\right\}$$ (14)

where, the matrix components are

$$m_{ij}(\tau) = \delta_{ij} + 2\gamma \sin(i\pi v_o \tau) \sin(j\pi v_o \tau)$$ (15)

$$c_{ij}(\tau) = 4\gamma (i\pi v_o) \sin(i\pi v_o \tau) \cos(j\pi v_o \tau)$$ (16)

$$k_{ij}(\tau) = n^4 \pi^2 \delta_{ij} - 2\mu(i\pi v_o)^2 \sin(i\pi v_o \tau) \sin(j\pi v_o \tau)$$
$$+ 2\mu(i\pi a_o) \sin(i\pi v_o \tau) \cos(j\pi v_o \tau)$$ (17)

$$f_i(\tau) = \gamma\pi^2 \left[\frac{\pi}{2} + v_0^2 \sum_{n=1}^{\infty} \frac{1-(-1)^n}{n^3} \sin(n\pi v_o \tau) \right.$$
$$\left. - a_o \sum_{n=1}^{\infty} \frac{1-(-1)^n}{n^4} \cos(n\pi v_o \tau) \right] \sin(i\pi v_o \tau)$$ (18)

The response of Eq. (14) may be analyzed using Runge-Kutta integration method.

2.2. Designing fuzzy controller

A general linear control theory is not applicable for the study since it is the time variant system and has a large non-linearity, as presented in Eq. (14). The fuzzy controller is effectively applicable for the study since the controller is designed by considering the characteristics of the vibration produced only, without taking into account the dynamic characteristics of the system.

The fundamental structure of the fuzzy controller applied to the simply supported beam carrying a moving mass is shown in Fig. 2.

The system output measured from the laser displacement sensor is transferred to the fuzzy set element by fuzzification. The decision making rule was properly designed by the controller designer based on the dynamic characteristics of the system to be studied. It produced the control input by defuzzifying the fuzzified output calculated from the measured values of the system.
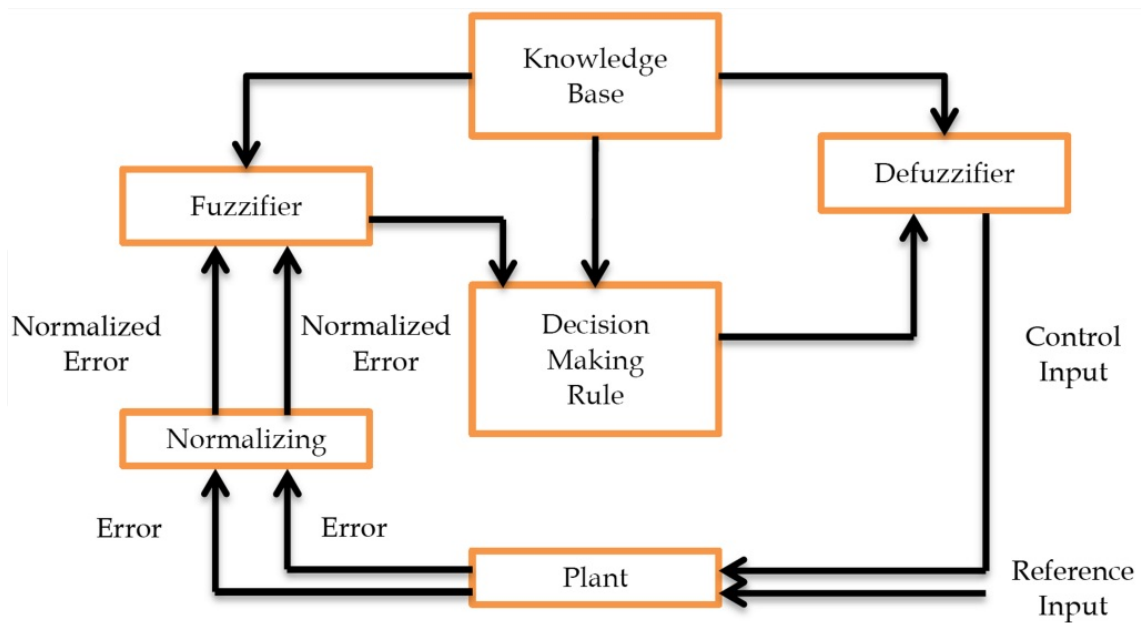
Figure 2. Flow-chart of fuzzy diagram.

The designer's experience, the professional's knowledge, and the dynamic characteristics of the system to be controlled are added by the designer in every process. The advantage of the fuzzy control theory using this type of design method is to design the controller easily when the characteristics or trends of the system are known or predictable to a certain extent, but the mathematical modelling for control is very difficult and complicated like the one for the study.

The system output obtained from the standardization process was fuzzified by formulating a fuzzy set. There are various ways to formulate a fuzzy set. A fuzzy set, which divides the range from -1 to 1 into 7 equal sections and has a triangular function as a membership function, was constructed and used for the present study as shown in Fig. 3.
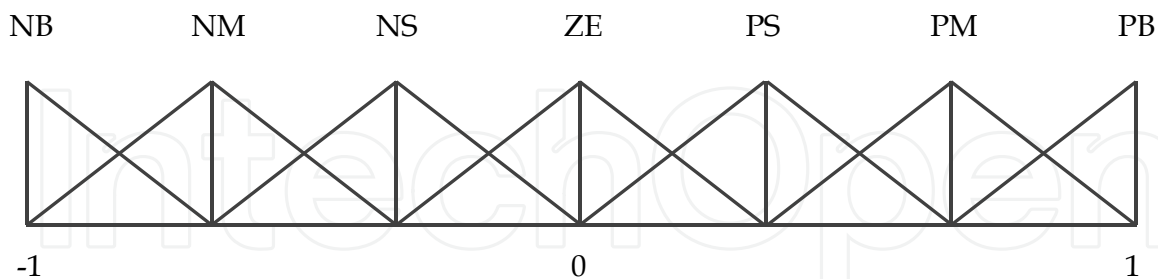
Figure 3. Fuzzy set with triangular membership function

It is desired to utilize the time response curve of a typical second-order system to a step input, as shown in Fig. 4, to determine the fuzzy rule for designing a fuzzy controller. At the point of "a", the control input should be PB(Positive Big) since the error is NB(Negative Big) and the time rate of the error is ZE(zero). At the point of "b", the control input is desired to be NS(Negative Small) if the error is ZE and the time rate of the error is PS(Positive Small). From the same logic, the control input at the point of "c" is needed to be PM(Positive Medium). Such a logical reasoning may be justified from the point of professional.
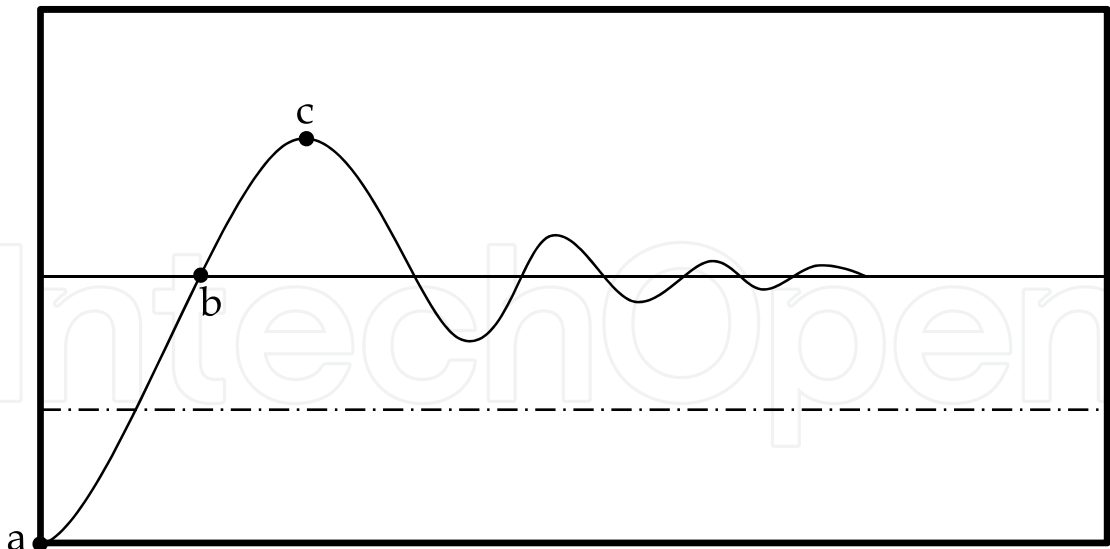
Figure 4. Typical response of controlled system.

		NB	NM	NS	ZE	PS	PM	PB
	NB	PB	PB	PM	PM	PS	PS	ZE
	NM	PB	PM	PM	PS	PS	ZE	NS
	NS	PM	PM	PS	PS	ZE	NS	NS
μ_e	ZE	PM	PS	PS	ZE	NS	NS	NM
	PS	PS	PS	ZE	NS	NS	NM	NM
	PM	PS	ZE	NS	NS	NM	NM	NB
	PB	ZE	NS	NS	NM	NM	NB	NB

The top header spans $\dot{\mu}_e$.

Table 1. Fuzzy rule with 7 elements

By expanding the logic stated above, the fuzzy rule may be constructed as shown in Table 1 for all cases of the fuzzy set consisted of seven elements.

where the errors e and $\dot{e}$ may be defined by the vibration displacement y, the vibration velocity $\dot{y}$, and the vibration displacement and the velocity to be controlled y_d and $\dot{y}_d$, respectively as follows

$$e = y - y_d \tag{19}$$

$$\dot{e} = \dot{y} - \dot{y}_d \tag{20}$$

The normalized error μ_e and $\dot{\mu}_e$ are defined by the initial target values y_o and $\dot{y}_o$ as

$$\mu_e = \frac{e}{y_o}, \qquad \dot{\mu}_e = \frac{\dot{e}}{\dot{y_o}} \qquad (21)$$

The actual control input was obtained by defuzzifying the fuzzified control input that was found based on the fuzzy rule from the normalized error and the time rate of the error obtained through the fuzzification process. For the study, the normalized control input was found by employing the min-max centroid method for the defuzzification.

3. Numerical analysis results of dynamic response to a moving mass

In order to produce numerical analysis results of dynamic response of a beam traversed by a moving mass, Runge-Kutta integration method was applied to Eq. (14). The dynamic deflection caused by a moving mass with constant velocity was investigated for the study, even though the dynamic deflection by a moving mass with constant acceleration can also be obtained from Eq. (14).
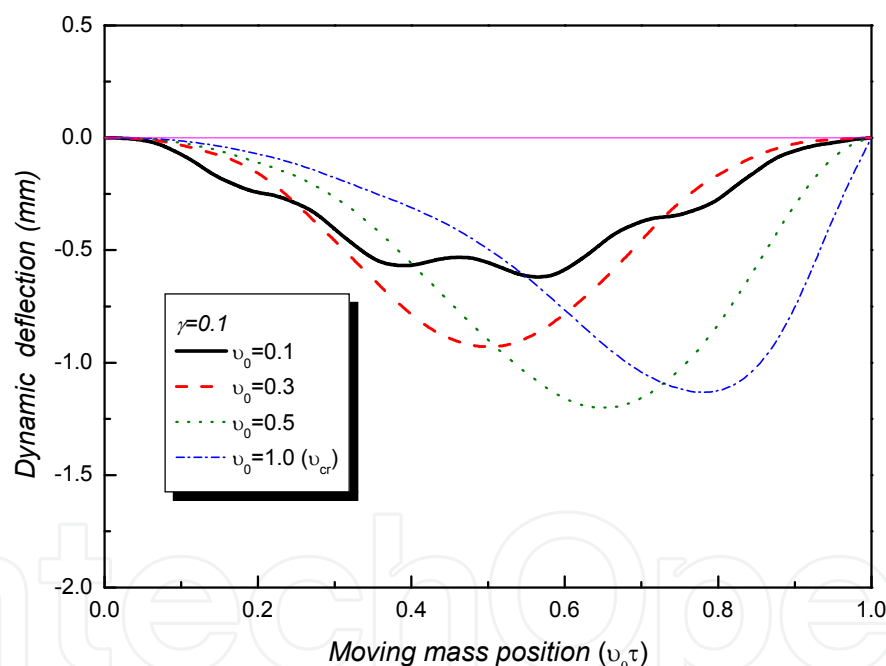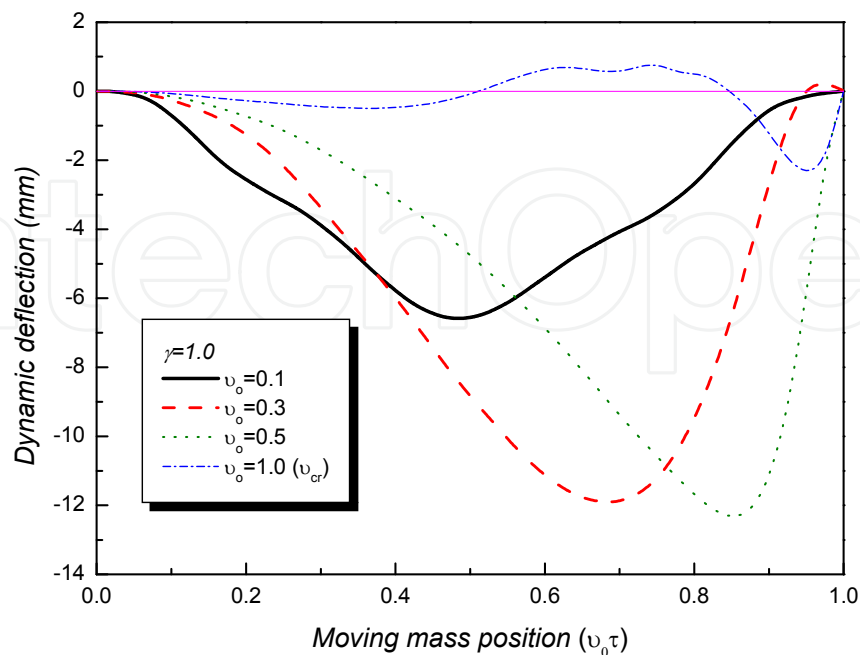

Figure 5. Dynamic deflection at the position of moving mass($v_o \tau$) for γ =0.1.

Figs. 5-7 show the dynamic responses at the dimensionless position $v_o\tau$ of the moving mass for the dimensionless velocity of the moving mass v_o =0.1, 0.3, 0.5, 1.0 when the mass ratio of the beam to the moving mass γ =0.1, 0.5, 1.0. Fig. 5 through Fig. 7 present the dynamic deflection only without including the static deflection. For γ =0.1, i.e. the mass of the beam is 1/10 of the mass of the moving mass, the first mode of an uniform beam was obtained as shown in Fig. 5, when the velocity of the moving mass is relatively low as v_o =0.1. For v_o ≥0.5, the location of the maximum deflection shifts to the right end of the beam, where the

moving mass arrives at. And also, the maximum dynamic deflection increases in general as the velocity of a moving mass increases. It is, however, observed that the maximum dynamic deflection decreases at the critical velocity v_{cr}. Fig. 6 of γ =0.5 through Fig. 7 of γ =1.0 show a similar trend to Fig. 5, but the difference from Fig. 5 is that the location of the maximum deflection shifts to the right end of the beam for all the velocity ranges from v_o =0.1 to the critical velocity as the velocity of a moving mass increases.
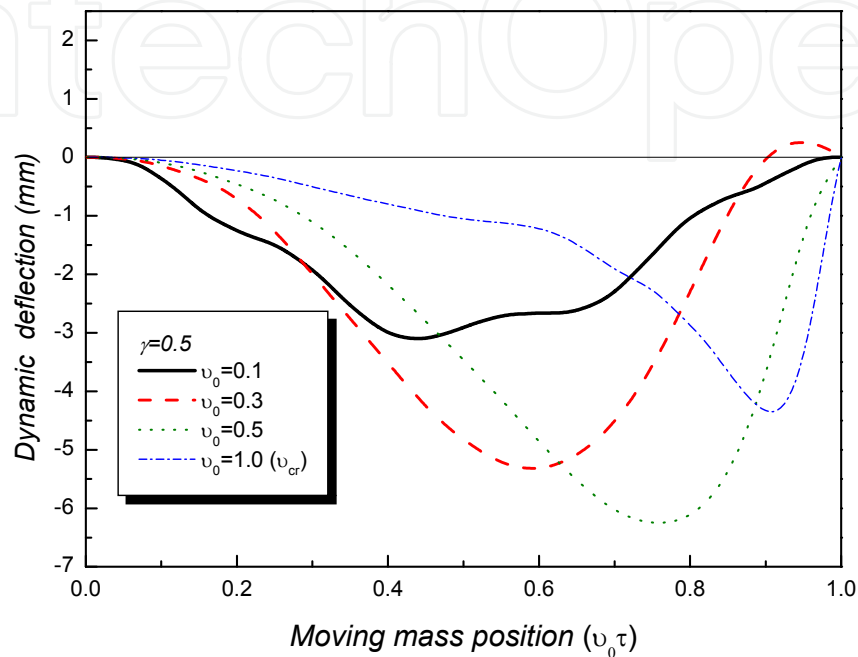
Figure 6. Dynamic deflection at the position of moving mass($v_o\tau$) for γ =0.5.

Figure 7. Dynamic deflection at the position of moving mass($v_o\tau$) for γ =1.0.
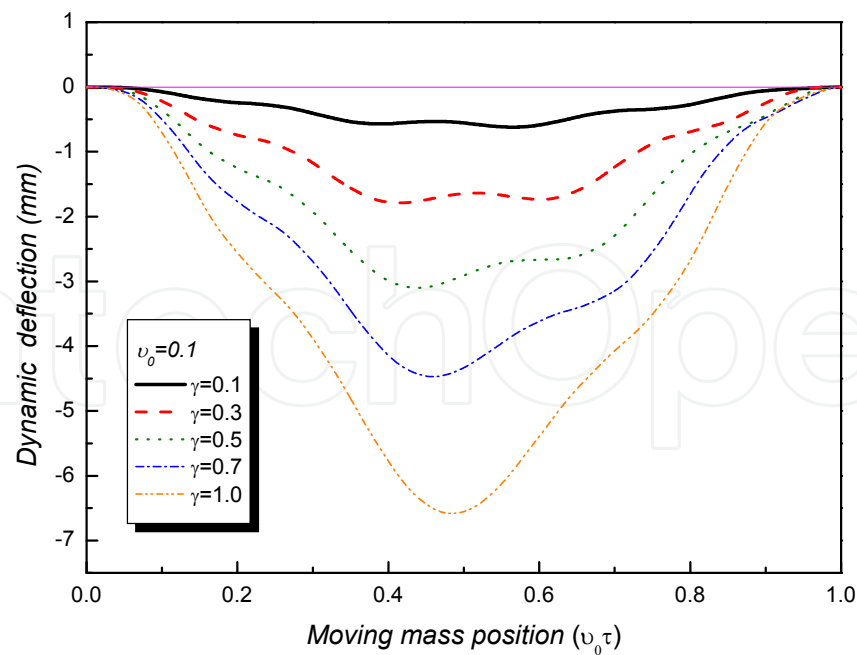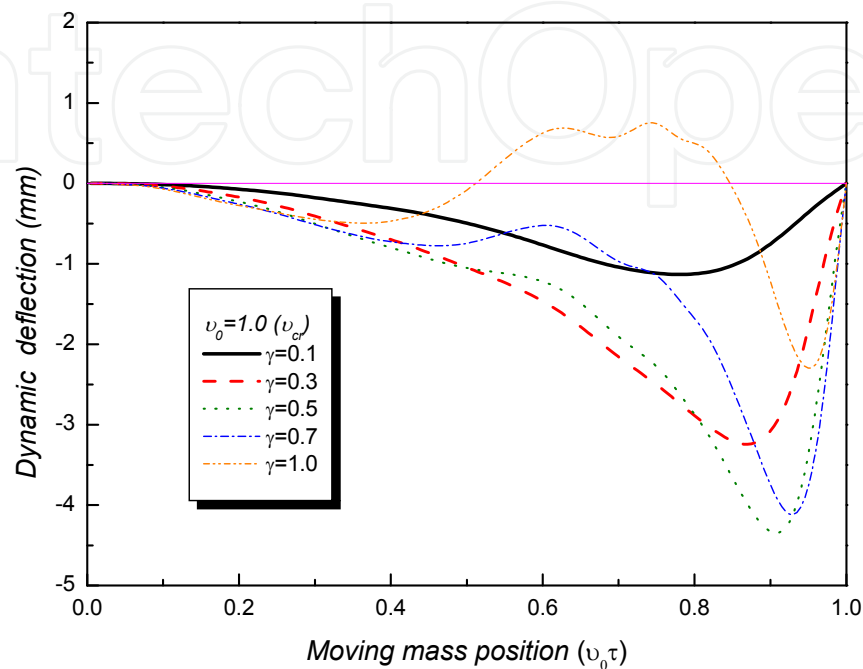
Figure 8. Dynamic deflection at the position of moving mass($v_o \tau$) for v_o =0.1
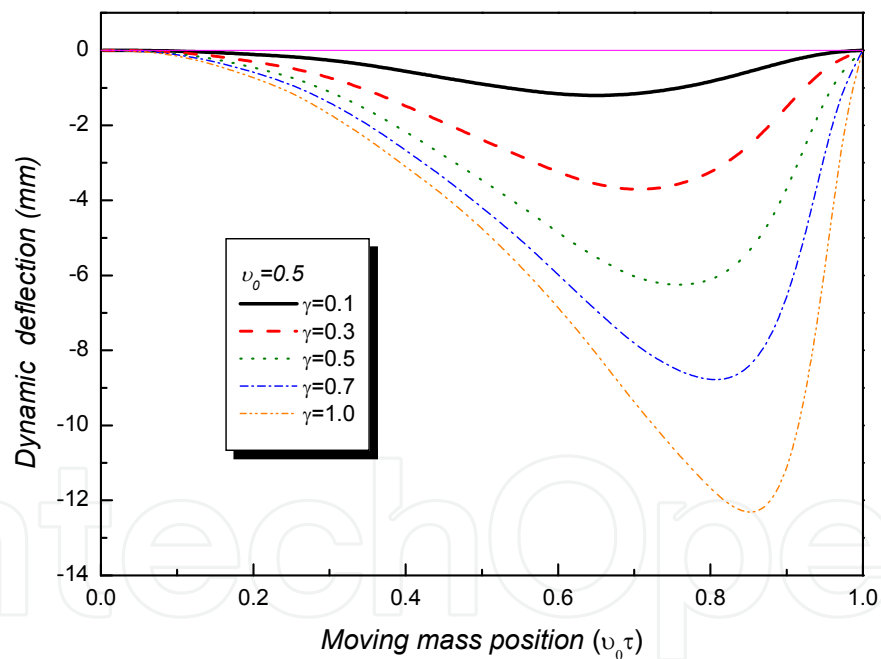

Figure 9. Dynamic deflection at the position of moving mass ($v_o \tau$) for v_o =0.5

Figs. 8-10 show the dynamic deflection at the dimensionless position of the moving mass for various mass ratios of γ when the dimensionless velocity of a moving mass v_o =0.3, 0.5, 1.0. When the velocity of the moving mass is as slow as v_o =0.1, the maximum dynamic deflection increases and its location slightly shifts to the right end as the mass ratio, γ, increases as shown in Fig. 8. And also, the moving mass position for the maximum deflection is near the middle point of the beam. For v_o =0.5 as shown in Fig. 9, the

maximum dynamic deflection increases and the moving mass position for the maximum dynamic deflection shifts to the right end as the mass ratio, γ, increases. For the critical velocity v_o =1.0 as shown in Fig. 10, however, the maximum dynamic deflection decreases as the mass ratio, γ, increases for ≥0.7 while the moving mass position for the maximum dynamic deflection still shifts to the right end of the beam.

Figure 10. Dynamic deflection at the position of moving mass ($v_o\tau$) for v_o =1.0
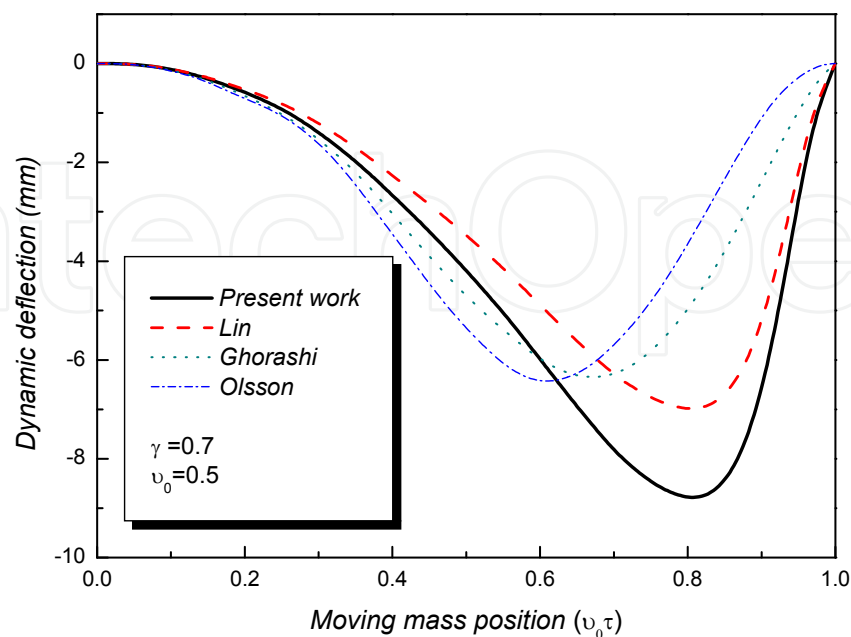
Figure 11. Comparison present results with other previous results for dynamic deflections (v_o =0.5)
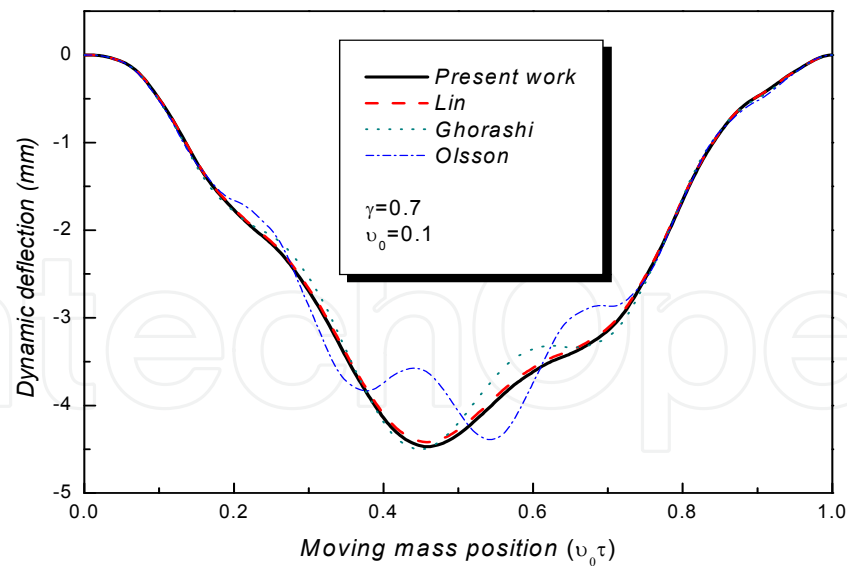
Figure 12. Comparison present results with other previous results for dynamic deflections (v_o =0.1)

Figs. 11 and 12 present the comparison of current results on the dynamic deflection and those from previous studies (references [6], [7], [8]) that do not consider as many effects of a moving mass as the present study does, for γ =0.7 and v_o =0.1, 0.5. As can be seen in these figures, the previous results are somewhat different from the present results. It is, therefore, believe that all the effects of a moving mass should be considered to predict more precisely the dynamic deflection of a beam traversed by a moving mass. This is confirmed by comparing with the experimental results presented in the Section 4.

## 4. Experimental apparatus and experiments

4.1. Experimental apparatus

An experimental apparatus was set up to control the dynamic deflection and the vibration of a simply supported uniform beam traversed by a moving mass as shown in Fig. 13.

The test beam has a groove along its length to help various sizes of a moving mass to run smoothly. The details of the test beam are shown in Table 2.

Material	Aluminum 6061
Modulus of Elasticity(Gpa)	7.07e+10
Density(kg / m^3)	2700
Mass(g)	283.0
Length (mm)	1000.0
Width (mm)	32.0
Thickness (mm)	4.0
Groove width (mm)	10.0
Groove depth (mm)	2.0

Table 2. Details of the test beam.
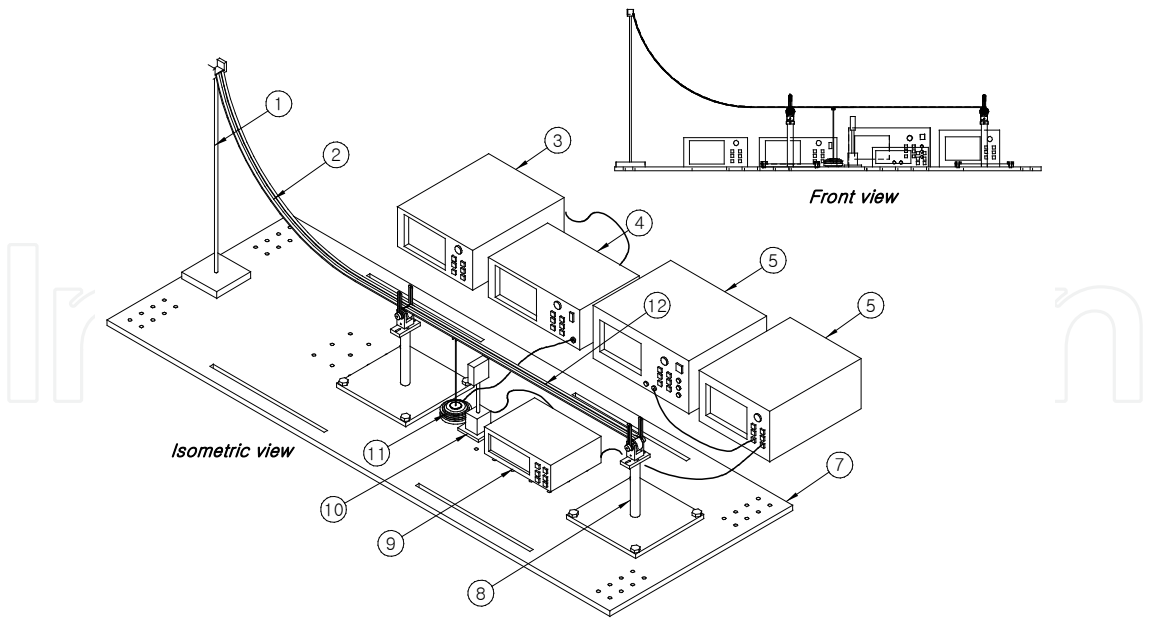
①Guide beam support pole ②Guide beam ③Power supply ④Amplifier ⑤FFT analyzer ⑥Digital oscilloscope ⑦Base ⑧Simply-supports ⑨Laser displacement meter ⑩Laser sensor ⑪Actuator ⑫Test beam

Figure 13. Experimental set up.

Steel balls were chosen as moving masses to reduce the friction with the test beam. The details of the moving masses are shown in Table 3

| Type of moving mass	Mass (g)	Diameter (mm)	Materials
M_1	67.0	25.35	
M_2	151.0	33.30	Steel
M_3	228.0	38.05	

Table 3. Details of the moving masses.

Photo. 1 depicts the experimental set-up for the study. A non-contact laser displacement sensor, a sensor controller, and a digital memory oscilloscope are installed to measure the dynamic response of the test beam traversed by a moving mass.

**Photo 1.** Photograph of experimental set-up.
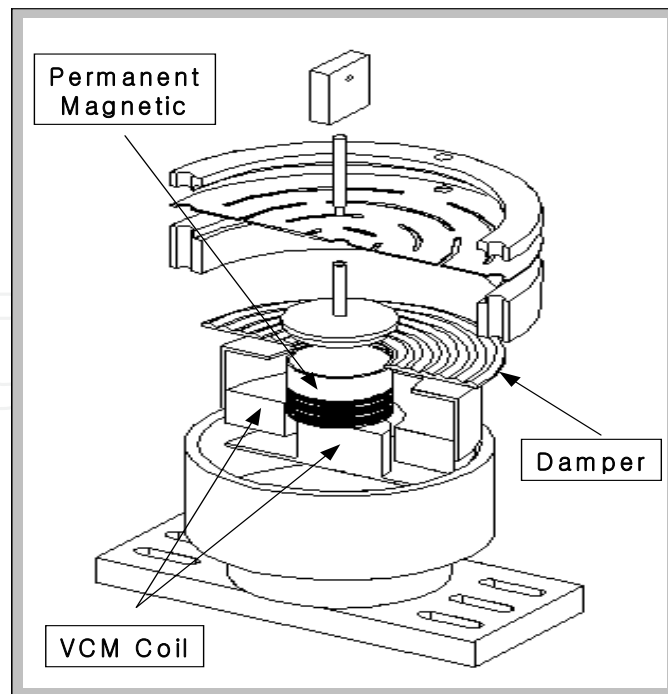
Figure 14. Schematic diagram of the front view of voice coil motor.
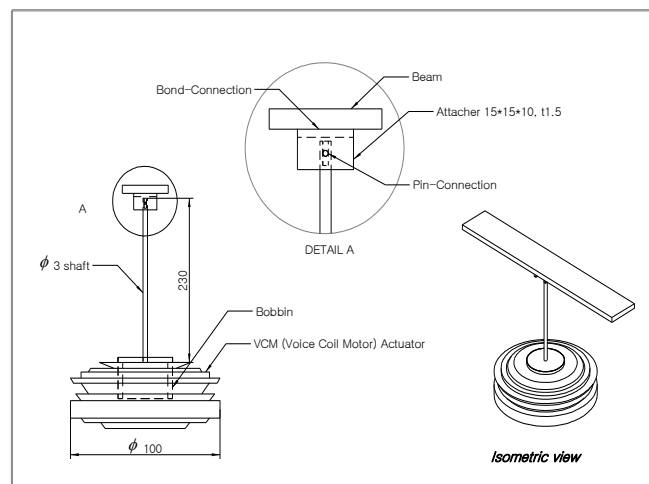
Figure 15. Details of a voice coil motor actuator.

Figs 14-15 show schematic diagram of the front view and details for the structure of a voice coil motor(VCM) actuator, respectively. The active actuator was reconstructed by using a commercial speaker. In the structure of the actuator, permanent magnet and voice coil wound in bobbin of the speaker were used, and an attacher and a shaft were produced in order to deliver control force from actuator to the beam. The actuator was built to suppress the dynamic deflection and the vibration of the test beam caused by a moving mass. The actuator is able to generate the control input by using a voice coil motor. The actuator is desired to be installed above and below the test beam to apply the force from the magnetic field to the beam. However, the control input is applied through a slender rod which connects the control actuator to the bottom of a beam, since the upper part of the beam should be free from any bar for a moving mass running. Photo. 2 depicts a test beam, moving masses and an actuator.
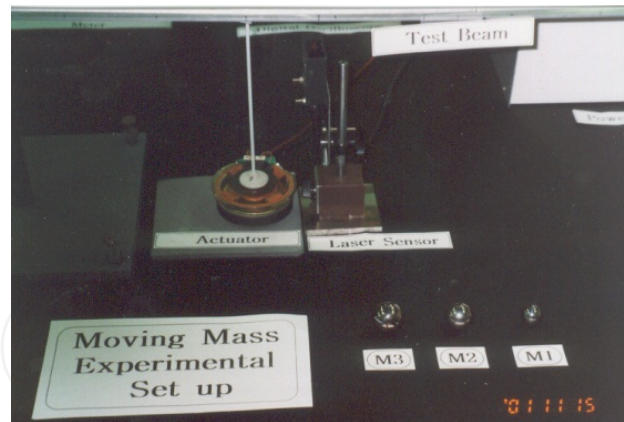
Photo 2.   Photograph of a test beam, moving masses and an actuator.

4.2. Experiments

Experiments are conducted to measure the dynamic response first, and then to control the vibration of a beam traversed by a moving mass. Three different mass ratios and three different velocity ratios of a moving mass were chosen to investigate the dynamic response of the system. The moving mass was released freely at the designated location of the guide beam and traveled the horizontal part of the guide beam of $210\,mm$ before entering and eventually passing through the test beam. The dynamic response was measured at $385\,mm$ from the entrance of the test beam by a non-contact laser displacement meter. The output signal was amplified before being monitored on an oscilloscope.

In order to suppress the dynamic deflection and vibration of a beam traversed by a moving mass, the control input is supplied by an actuator as shown in Fig. 13. The control input in accordance with the fuzzy logic is applied to the system through a voice coil motor at the same time when the moving mass enters the test beam. The signal of the dynamic response was amplified by an amplifier and then displayed on an oscilloscope.

Such experiments on the dynamic deflection and the vibration control were performed in order for the selected masses and velocities of moving masses. The details of the moving mass used are shown in each figure.

## 4.3. Experimental results and discussion

4.3.1 Experimental results of the dynamic response and discussion

Figs. 16-18 present both the experimental results and the analytical results from the numerical simulation on the dynamic response of a simply supported beam traversed by a moving mass. Figs. 16-18 show both analytical and experimental results on the dynamic response for three different velocities and magnitudes of a moving mass (v =1.299(m / s), v =1.880(m / s), v =2.450(m / s), M =67(g), M =151(g), M =228(g)).

The analytical results agree well with the experimental results in both the magnitude and the shape of the dynamic response curve for two velocities(v =1.299(m / s), v =1.880(m / s))

of a moving mass. For v =2.450(m/s), however, analytical and experimental results are somewhat different as shown in Fig. 18. It is thought that the difference becomes greater as a higher velocity of a moving mass produces a stronger impact at the joint of the guide beam and the test beam. For the residual vibration region, two different initial conditions of which the moving mass leaves the beam are believed to make the difference between two results as explained previously.
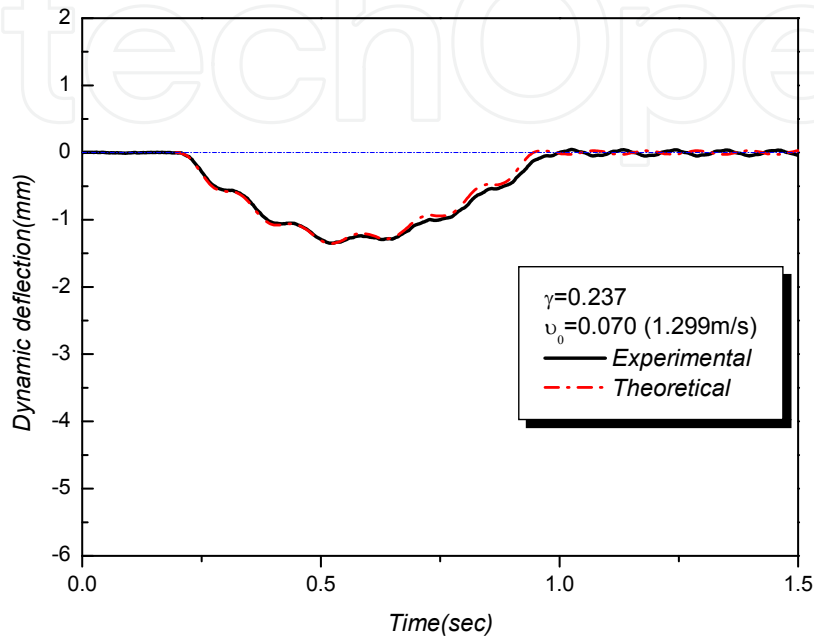
Figure 16. Comparison theoretical results with experimental ones for beam deflections (γ =0.237 and v_o =0.07)
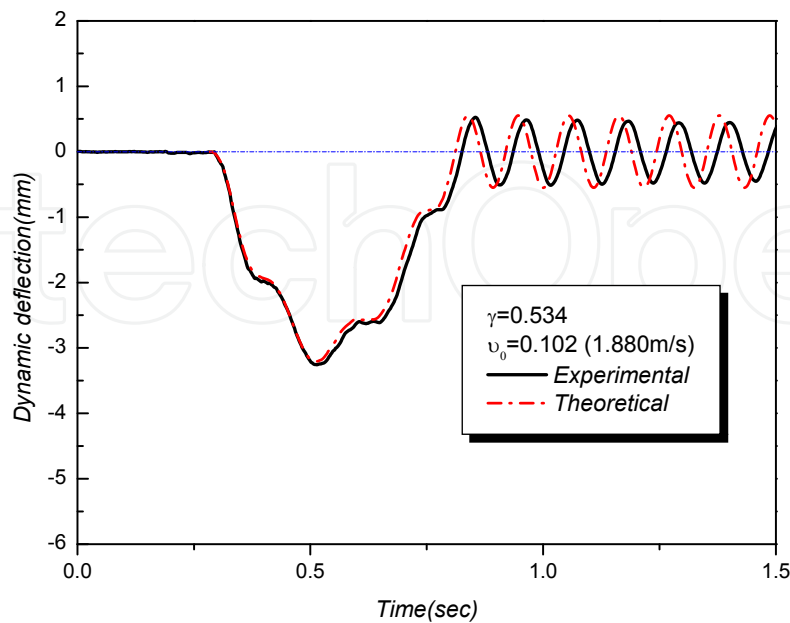

Figure 17. Comparison theoretical results with experimental ones for beam deflections (γ =0.534 and v_o =0.102)
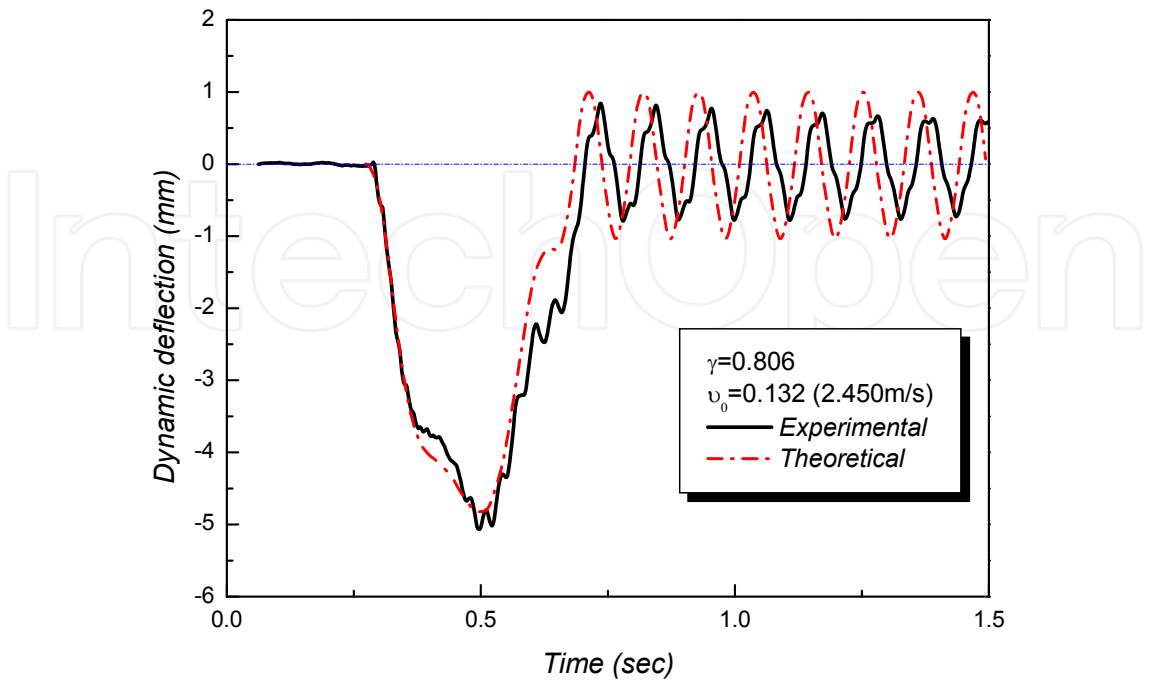
Figure 18. Comparison theoretical results with experimental ones for beam deflections (γ =0.806 and v_o =0.132)

4.3.2. Experimental results of vibration control of a beam

A control using a voice-coil motor was conducted to suppress the amplitude of dynamic response and vibration of a beam traversed by a moving mass. The Matlab simulation was performed to find the best location of the actuator for the control input.
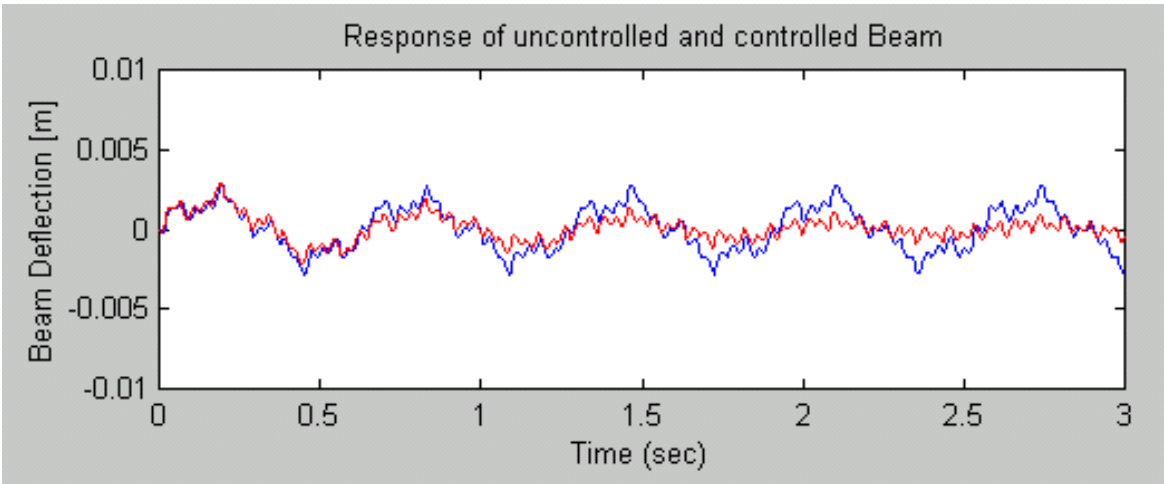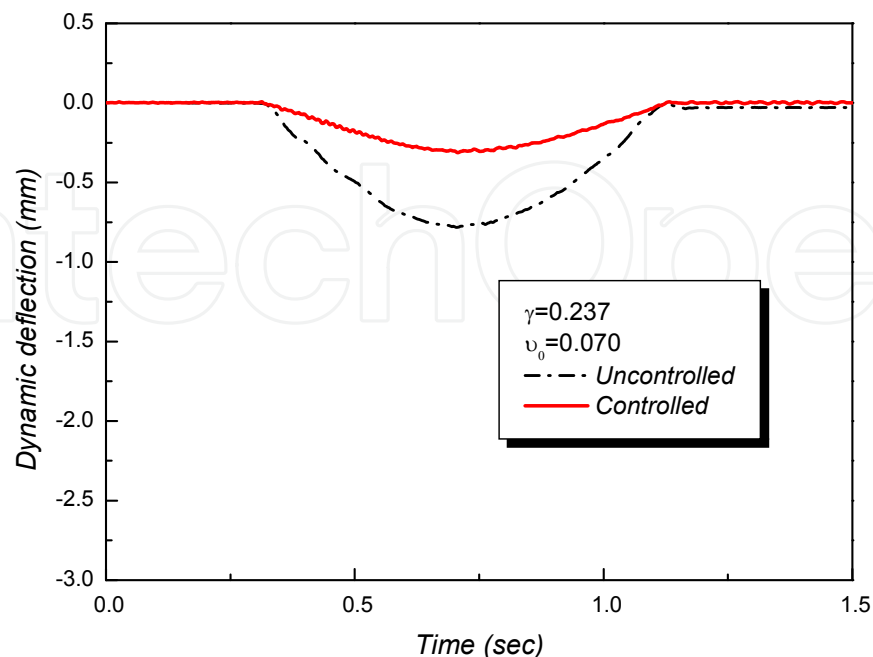

Figure 19. Response of uncontrolled and controlled beam for arbitrary disturbances (actuator position = l /10)

The results are presented in Figs. 19-20. The simulation was performed by investigating the response to the disturbance applied to a certain point for various locations of the actuator. Two typical simulation results are presented in Figs. 19-20. As shown in these figures, a better controlled result was obtained when the actuator is located at 3/10 of the beam length l. And also, the node of the third mode is believed to be a good place for locating the actuator since it is intended to control up to the second mode for the study. The position of 3/10 of the beam length l from the entrance of the test beam was finally selected for the location of the actuator. The experiments for control were conducted after locating the actuator at $3l/10$ based on the simulation results shown in Figs. 19 and 20.
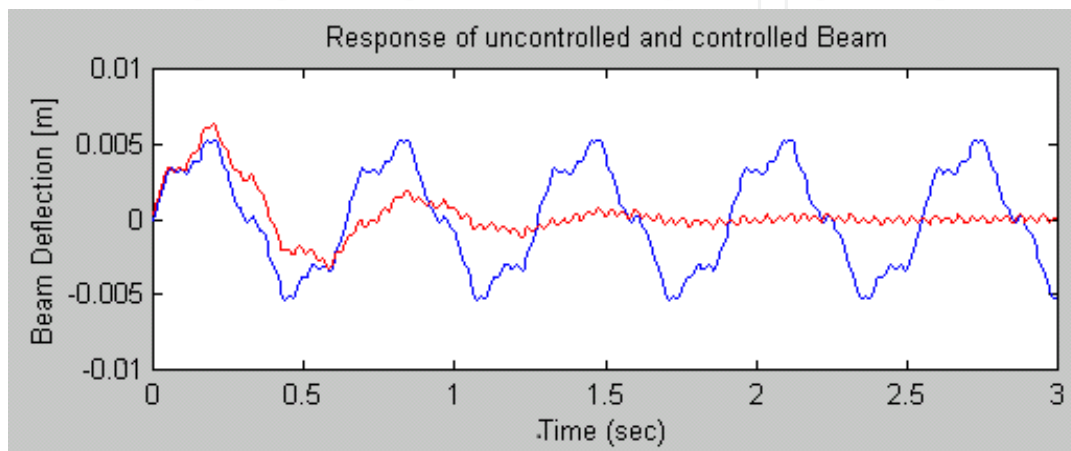
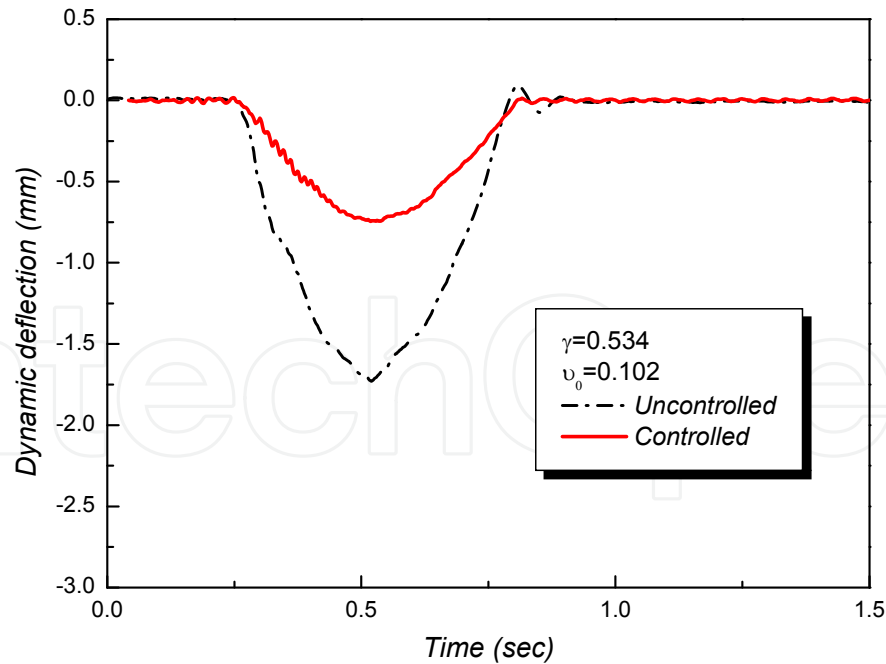**Figure 20.** Response of uncontrolled and controlled beam for arbitrary disturbances (actuator position = $3l/10$)

Figure 21. Dynamic deflections of uncontrolled and controlled beam for γ =0.237 and v_o =0.07.

The experimental results under both uncontrolled and controlled conditions are presented in Figs. 21-23.

The experimental results of the dynamic deflection in 4.3.1 and the test results for the uncontrolled case in 4.3.2 are supposed to be identical for the same mass ratio γ and velocity ratio v_o. But they are different because the stiffness and the damping provided by the slender rod that connects the actuator and the beam change the dynamic characteristics of the system.

Therefore, it is necessary to include the slender rod to simulate the dynamic deflection curve for the uncontrolled cases shown in Figs. 21-23. It is, however, very difficult to develop the mathematical governing equation for such a system. Thus, the present study focuses on the control effect only by applying the control input from the measured dynamic responses of the system with the control actuator.

For three different velocities(v =1.299(m/s), v =1.880(m/s), v =2.450(m/s)), in general, the dynamic deflections are controlled to be less than 50% of the uncontrolled ones. And also, it does help to suppress the residual vibration occurred after the moving mass passes through the beam.

Figure 22. Dynamic deflections of uncontrolled and controlled beam for γ =0.534 and v_o =0.102.
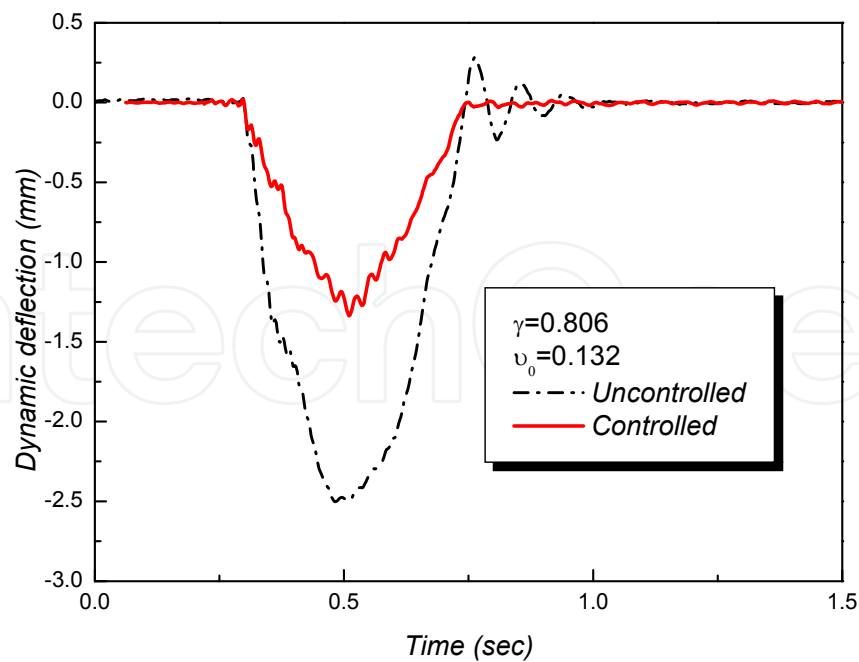
Figure 23. Dynamic deflections of uncontrolled and controlled beam for γ =0.806 and v_o =0.132.

5. Conclusion

The following results were obtained from the fuzzy control studies on the dynamic response and the vibration of a simply supported beam traversed by a moving mass with a constant velocity. Firstly, the position of a moving mass at the maximum dynamic deflection moves to the right end of a beam as the mass ratio of a moving mass γ increases for a lower velocity ratio of a moving mass v_o than the critical velocity. Secondly, the position of a moving mass at the maximum dynamic deflection moves to the right end of a beam as the velocity of a moving mass increases for a given mass ratio of a moving mass γ.

Thirdly, the experimental results of the dynamic deflection of a beam traversed by a moving mass agree well with the simulation results.

Fourthly, the dynamic deflection and the residual vibration of a beam traversed by a moving mass were successfully reduced more than 50 % through the fuzzy control.

Author details

Bong-Jo Ryu and Yong-Sik Kong
Hanbat National University / Hanwha L&C, South Korea

6. References

[1] Strokes, G. G. (1849). Discussion of a Differential Equation Relation to the Breaking of Rail Way Bridges. *Transactions of the Cambridge Philosophical Society*, Vol.85, pp.707-735.

[2]   Ayre, R. S.; Ford, G. & Jacopsen, L. S. (1950). Transverse Vibration of a Two Span Beam under Action of Moving Constant Force. *Transactions of the ASME, Journal of Applied Mechanics*, Vol.17, pp.1-2.

[3]   Yoshida, D. M. & Weaver, W. (1971). Finite Element Analysis of Beams and Plates with Moving Loads. *Publication of International Association for Bridge and Structural Engineering*, Vol. 31, No. 1, pp.179-195.

[4]   Ryu, B. J. (1983). Dynamic Analysis of a Beam Subjected to a Concentrated Moving Mass, Master Thesis, Yonsei University, Seoul, Korea.

[5]   Sadiku, S. & Leipholz, H. H. E. (1987). On the Dynamics of Elastic Systems with Moving Concentrated Masses. *Ingenieur-Archiv*, Vol. 57, pp. 223-242.

[6]   Olsson, M. (1991). On the Fundamental Moving Load Problem. *Journal of Sound and Vibration*, Vol. 145, No. 2, pp. 299-307.

[7]   Esmailzadeh, E. & Ghorashi, M. (1992). Vibration Analysis of Beams Traversed by Moving Masses, *Proceedings of the International Conference on Engineering Application of Mechanics*, Vol. 2, pp. 232-238, Tehran, Iran.

[8]   Lin, Y. H. (1997). Comments on Vibration Analysis of Beams Traversed by Uniform Partially Distributed Moving Masses. *Journal of Sound and Vibration*, Vol. 199, No. 4, pp. 697-700.

[9]   Wang, R. T. & Chou, T. H. (1998). Nonlinear Vibration of Timoshenko Beam due to a Moving Force and the Weight of Beam. *Journal of Sound and Vibration*, Vol. 218, No. 1, pp. 117-131.

[10] Wu, J. J. (2005). Dynamic Analysis of an Inclined Beam due to Moving Load. *Journal of Sound and Vibration*, Vol. 288, pp. 107-131.

[11] Abdel-Rohman, M. & Leipholz, H. H. E. (1980). Automatic Active Control of Structures, North-Holland Publishing Co. & Sm Publications.

[12] Kwon, H. C.; Kim, M. C. & Lee, I. W. (1998). Vibration Control of Bridges under Moving Loads. *Computers and Structures*, Vol. 66, pp. 473-480.

[13] Ryou, J. K.; Park, K. Y. & Kim, S. J. (1997). Vibration Control of Beam using Distributed PVDF Sensor and PZT Actuator. *Journal of Korean Society of Noise and Vibration Engineering*, Vol. 7, No. 6, pp. 967-974.

[14] Bailey, T. & Hubbard Jr., J. E. (1985). Distributed Piezoelectric-Polymer Active Vibration Control of a Cantilever Beam. *Journal of Guidance, Control, and Dynamics*, Vol. 8, No.5, pp.605-611.

[15] Kwak, M. K. & Sciulli, D. (1996). Fuzzy-Logic Based Vibration Suppression Control Experiments on Active Structures. *Journal of Sound and Vibration*, Vol. 191, No. 1, pp.15-28.

[16] Sung, Y. G. (2002). Modeling and Control with Piezo-actuators for a Simply Supported Beam under a Moving Mass. *Journal of Sound and Vibration*, Vol. 250, No. 4, pp.617-626.

[17] Nikkhoo, A.; Rofooei, F. R. & Shadnam, M. R. (2007). Dynamic Behavior and Modal Control of Beams under Moving Mass. *Journal of Sound and Vibration*, Vol. 306, pp. 712-724.

[18] Prabakar, R. S.; Sujatha, C. & Narayanan, S. (2009). Optimal Semi-active Preview Control Response of a Half Car Vehicle Model with Magneto-rheological Damper. *Journal of Sound and Vibration*, Vol. 326, pp. 400-420.

[19] Pisarski, D. & Bajer, C. I. (2010). Semi-active Control of 1D Continuum Vibrations under a Travelling Load. *Journal of Sound and Vibration*, Vol. 329, pp. 140-149.